
Intrathecal CRISPR-edited allogeneic IL-13Ra2 CAR T Cells for recurrent high-grade Glioma: preclinical characterization and phase I trial

Received: 11 September 2025

Accepted: 18 December 2025

Cite this article as: Li, X., Shang, X., Liu, J. *et al.* Intrathecal CRISPR-edited allogeneic IL-13Ra2 CAR T Cells for recurrent high-grade Glioma: preclinical characterization and phase I trial. *Nat Commun* (2025). <https://doi.org/10.1038/s41467-025-68112-6>

Xuetao Li, Xiaoyun Shang, Jiangang Liu, Yang Zhang, Xian Jia, Huabing Li, Yihan Wang, Jianen Gao, Xu Ma, Xuewen Zhang, Xiaoci Rong, Wenjuan Gan, Yu Zhang, Jie Chen, Lin Wang, Zhen Bao, Liang He, Xigang Yan, Yang Liu, Jie Shao, Zongyu Xiao, Zhiming Wang, Haiping Zhu, Zhong Wang, Yuzhang Wu & Yulun Huang

We are providing an unedited version of this manuscript to give early access to its findings. Before final publication, the manuscript will undergo further editing. Please note there may be errors present which affect the content, and all legal disclaimers apply.

If this paper is publishing under a Transparent Peer Review model then Peer Review reports will publish with the final article.

Intrathecal CRISPR-Edited Allogeneic IL-13Ra2 CAR T Cells for Recurrent High-Grade Glioma: Preclinical Characterization and Phase I Trial

Xuetao Li^{1#}, Xiaoyun Shang^{2#}, Jiangang Liu^{3#}, Yang Zhang^{1#}, Xian Jia^{2#}, Huabing Li⁴, Yihan Wang^{5,6}, Jianen Gao^{5,6}, Xu Ma^{5,6}, Xuewen Zhang¹, Xiaoci Rong¹, Wenjuan Gan⁷, Yu Zhang⁸, Jie Chen⁹, Lin Wang¹⁰, Zhen Bao¹, Liang He¹, Xigang Yan¹¹, Yang Liu¹, Jie Shao¹, Zongyu Xiao¹, Zhiming Wang¹, Haiping Zhu¹, Zhong Wang^{3*}, Yuzhang Wu^{12*}, Yulun Huang^{1,3*}

Affiliations:

¹ Department of Neurosurgery, The Fourth Affiliated Hospital of Soochow University, Suzhou, China.

² T-Maximum Pharmaceutical (Suzhou) Co., Ltd., Suzhou, China.

³ Department of Neurosurgery, The First Affiliated Hospital of Soochow University, Suzhou, China.

⁴ Medical Center on Aging, Center for Immune-Related Diseases at Shanghai Institute of Immunology, Ruijin Hospital, Shanghai Jiao Tong University School of Medicine, Shanghai, China.

⁵ National Research Institute for Family Planning, Beijing, China.

⁶ National Human Genetic Resources Center, Beijing, China.

⁷ Department of Pathology, The Fourth Affiliated Hospital of Soochow University, Suzhou, China.

⁸ Department of Radiology, The Fourth Affiliated Hospital of Soochow University, Suzhou, China.

⁹ Department of Radiotherapy, The Fourth Affiliated Hospital of Soochow University,

Suzhou, China.

¹⁰ Center of Clinical Laboratory, The Fourth Affiliated Hospital of Soochow University,

Suzhou, China.

¹¹ Department of Neurosurgery, Suzhou Wuzhong people's Hospital, Suzhou, China.

¹² Army Medical University, Chongqing, China.

These authors contributed equally: Xuetao Li, Xiaoyun Shang, Jiangang Liu, Yang Zhang, Xian Jia.

E-mail: Yulun Huang: huangyulun@suda.edu.cn;

Zhong Wang: W13306208761@163.com;

Yuzhang Wu: wuyuzhang@iicq.vip

1 **Abstract**

2 Patients with recurrent high-grade glioblastoma have a median survival of 6-8 months,
3 with limited therapeutic options. In recent years, interest has grown in applying
4 chimeric antigen receptor T (CAR-T) cells to solid cancers, including advanced gliomas.
5 Here we generated off-the-shelf CRISPR-Cas9-edited IL-13Ra2-specific allogeneic
6 universal CAR-T cells (MT026) by disrupting the endogenous TCR to prevent graft-
7 versus-host disease and knocking out HLA class I molecules to mitigate the host-
8 versus-graft response, and observed minimal NK-cell-mediated rejection in preclinical
9 studies. In a first-in-human, single-center, open-label investigator-initiated trial
10 (ChiCTR2000028801) in patients with high-grade glioma with prior therapy failure and
11 short life expectancy, intrathecal injection of MT026 via lumbar puncture (1.0-
12 3.0×10^7 cells per dose) demonstrated favorable tolerability and safety (primary
13 outcome), pharmacokinetic characteristics, and preliminary clinical activity (secondary
14 outcomes). Among the five patients enrolled, one achieved a complete response and
15 three achieved partial responses. No grade ≥ 3 adverse events were observed; the
16 predominant treatment-related toxicities were grade 1-2 pyrexia, hypoxia, and vomiting.
17 Trial enrolment was halted after enrolment of the first five patients, however these
18 preliminary clinical data support the potential benefit of locally administered allogeneic
19 universal CAR-T cell therapy for recurrent glioblastoma.

20

21 **Introduction**

22 Glioblastoma accounts for over 49.1% of newly diagnosed primary brain malignancies
23 each year [1]. The current standard of care for glioblastoma includes maximal safe
24 surgical resection followed by radiation, chemotherapy with temozolomide, and tumor-
25 treating fields [2, 3]. However, nearly all glioblastomas relapse after standard-of-care

26 treatment, and patients survive only 25-30 weeks [4]. For recurrent disease, standard-
27 of-care options are suboptimal, and effective therapeutic approaches remain to be
28 established. Therefore, patient participation in clinical trials is recommended per the
29 NCCN guideline [2].

30 Administration of chimeric antigen receptor T (CAR-T) cells into the CSF allows
31 bypassing the blood–brain barrier and may help overcome the immunosuppressive
32 glioma microenvironment by delivering a preponderant supply of tumor-specific T cells
33 to immunologically “cold” gliomas, which kill tumor cells by homing to tumor-
34 associated antigens [5].

35 IL-13Ra2, expressed in over 75 % of glioblastomas and associated with increased
36 tumor invasiveness and poor prognosis, is a well-recognized CAR-T target [5-8].

37 Intrathecal administration of autologous CAR-T cells targeting IL-13Ra2 for
38 glioblastoma has been reported with favorable tolerance and tumor regression in a
39 single patient [9]. However, autologous T cell immunotherapy for glioblastoma may
40 face obstacles due to suboptimal T cell quality and quantity. The patient-specific nature
41 and complex manufacturing process make autologous cell generation costly and time-
42 consuming. The fact that patients with recurrent high-grade glioma have survival
43 measured in months in the absence of effective therapies [10, 11] calls for more efficient
44 CAR-T production. Developing off-the-shelf, on-demand allogeneic CAR-T to
45 overcome exhaustion and preserve effector function and persistence is desirable to
46 achieve complete clinical potential.

47 Nevertheless, intrinsic TCRs on allogeneic T cells can recognize recipient alloantigens,
48 which may result in graft-versus-host disease (GvHD). In addition, expression of HLA
49 molecules on the surface of allogeneic T cells can trigger prompt rejection by the host
50 immune system through host-versus-graft reaction (HvGR) [12].

51 Recent advances in genome-editing technologies have greatly expanded the ability to
52 modify genomic sequences as desired [13-15]. The Major Histocompatibility complex
53 class I (MHC-I), known as human leukocyte antigen class I (HLA-I), includes the
54 classical HLA-A, HLA-B, and HLA-C molecules. HLA matching affects clinical
55 outcomes of hematopoietic stem cell transplantation [16]. Numerous studies have
56 aimed to generate hypoimmunogenic induced pluripotent stem cells or to refine
57 hematopoietic stem cell transplantation (HSCT) to minimize immune rejection caused
58 by HLA-type mismatches [17-20].

59 To modulate immune responses mediated by T cells, NK cells, and macrophages against
60 transferred cells, researchers have tested knocking out beta 2-microglobulin (B2M) to
61 eliminate HLA class I surface expression, knocking out CIITA to inhibit MHC class II
62 expression, and overexpressing HLA-E and CD47 to reduce NK- and macrophage-
63 mediated rejection [17, 19–21]. The primary challenges in employing allogeneic T cells
64 are GvHD and HvGR. The former can be mitigated by removing the TCR, typically
65 achieved through knockout (KO) of the constant domain in either the α or β chain, or
66 by substituting specific TCR components to impair antigen recognition [22]. Although
67 disruption of the common subunit β 2-microglobulin (B2M) completely prevents HLA-
68 I surface expression, it may render the cell susceptible to NK-cell lysis [23]. However,
69 knocking out specific subunits of HLA-I molecules alone still carries the risk of host T
70 cell attacks against the remaining HLA molecules. Novel approaches to bypass
71 surveillance by the host immune system of allogeneic universal CAR-T (UCAR-T) cells
72 have been intensively investigated [12, 19, 24, 25].

73 Here, we successfully generated MT026 by knocking out *TRAC* and disrupting HLA-I
74 α chains, enabling control of GvHD and mitigation of HvGR. We present an alternative
75 research approach and show that disruption of most HLA class I molecules enhances

76 the persistence of IL-13R α 2-specific allogeneic CAR-T cells in patients with recurrent
77 glioblastoma. Data from a first-in-human, single-center, open-label investigator-
78 initiated trial (IIT; ChiCTR2000028801) using CRISPR-Cas9-edited universal CAR-T
79 therapy, delivered intrathecally to tumor sites, demonstrated favorable tolerability,
80 safety, pharmacokinetic (PK) characteristics, and preliminary efficacy of IL-13R α 2-
81 targeted allogeneic UCAR-T therapy.

82

83 **Results**

84 ***Preparation and characterization of allogeneic UCAR-T cells***

85 We initially generated allogeneic UCAR-T cells by transducing a lentiviral vector
86 encoding an anti-IL-13R α 2 CAR into CD3-positive T cells. To minimize both GvHD
87 and HvGR in recipients of allogeneic UCAR-T cells, we designed four sgRNAs
88 targeting the first exon of the *TRAC* gene and multiple sgRNAs for the HLA-I α chain,
89 rather than the B2M gene, in PBMCs from an HLA-A2-positive donor. Cas9/sgRNA
90 RNP complexes were electroporated, and we screened for the single sgRNA that
91 produced the highest disruption efficiency. Finally, multiple batches suitable for clinical
92 use were stably manufactured after process development and optimization
93 (**Supplementary Table 1**). Vector copy number (VCN) analysis showed an average of
94 1.13 ± 0.38 integrations in UCAR-T cells (**Supplementary Fig. 1a-d**). Surface
95 expression levels of TCR and HLA-I, as well as the phenotype, were confirmed by flow
96 cytometry to be marginal. The percentage of CAR-positive cells was 45.3%, and the
97 percentages of *TRAC* knockout (by CD3-negative staining) and HLA-I knockout (by
98 HLA-ABC staining) were 99.52 % and 95.23 %, respectively (**Fig. 1a; Supplementary**
99 **Fig. 1c**). Moreover, expression of the early activation markers CD69 and CD137 was
100 assessed *in vitro* following co-culture with U251 target cells to determine the activation

101 level of allogeneic UCAR-T cells. The flow cytometry data indicated that double
102 knockout of TCR and HLA-I enabled activation by target cells (**Fig. 1b**).

103

104 ***Off-target activity assessment***

105 To address concerns about off-target specificity and chromosomal stability of the dual
106 TRAC-HLA CRISPR-Cas9-edited MT026 product, we used orthogonal genome-wide
107 profiling methods (AID-seq, PEM-seq, GUIDE-seq, and iGUIDE-seq) to
108 systematically characterize genetic perturbations.

109 AID-seq identified 465 (*Sg1/TRAC*) and 1,491 (*Sg2/HLA*) putative off-target sites
110 (**Supplementary Table 2**), with no overlap across sgRNA-specific loci. GUIDE-seq
111 and iGUIDE-seq detected minimal off-target editing in dual-edited samples (sample 1:
112 56–62 sites; sample 2: 41–56 sites), with only one coding-region hit (MUC4; <0.1%
113 clone fraction) indicating negligible oncogenic risk. Single-gene-edited controls
114 (*TRAC*: 106–129 sites; *HLA*: 42–48 sites) showed comparable off-target profiles,
115 confirming specificity that is independent of sgRNA.

116 PEM-seq revealed low-frequency translocations at on-target loci (*TRAC*: 10.62%, *HLA*:
117 1.79 %). No individual translocation event exceeded a mutation frequency of 5 %, and
118 none involved cancer-related genes (**Supplementary Table 3**). A notable 4.4 %
119 translocation frequency at the CD8 locus was excluded from analysis due to junctional
120 criteria but warrants clinical monitoring for functional impact.

121 Amplicon sequencing with CRISPResso2 analysis (20-bp quantification window \pm 10
122 bp from cut sites) confirmed 100 % on-target editing specificity in dual-edited MT026
123 cells (samples 1 and 2), with no detectable off-target modifications in flanking regions
124 (**Supplementary Table 4**). Collectively, these multilayered assessments demonstrate:
125 1) sgRNA-specific off-target profiles with limited coding region impact, 2) low

126 structural variation risk at therapeutic thresholds, and 3) precise on-target editing,
127 supporting the safety and clinical translatability of this dual-edited UCAR-T product.

128

129 ***Evaluation of the Effects of HLA-TRAC Dual-Editing Strategy on TCR and HLA-I***
130 ***Functions***

131 To validate the efficacy of the *HLA-TRAC* dual-editing strategy in mitigating GvHD
132 and HvGR risks, we systematically evaluated the functional consequences of TCR and
133 HLA-I disruption.

134 To verify the protective role of the *HLA-I* gene-editing strategy, we used allogeneic NK
135 cells with IL-2 to enhance NK function. UCAR-T cells were co-cultured with NK cells
136 for 24 h. Only 20–30 % of UCAR-T cells were lysed by NK cells, whereas the positive-
137 control cell line K562, which lacks HLA-I expression, exhibited ~60 % lysis. As
138 expected, WT T cells with HLA-I expression resisted killing (**Fig. 1c**). In order to
139 further evaluate whether the dual knockout allogeneic UCAR-T cells would induce
140 GvHD on recipients as well as HvGR, which were the common issues of allogeneic
141 UCAR-T cells, UCAR-T generated by different knockout strategies were challenged
142 by allogeneic PBMCs. MT026 cells (TCR-knockout UCAR-T) showed no proliferation
143 when co-cultured with allogeneic PBMCs, in stark contrast to conventional CAR-T
144 cells (TCR-intact) and WT T cells, which exhibited significant activation and expansion
145 (**Fig. 1d**).

146 For HvGR evaluation, we conducted co-culture experiments using cells with different
147 knockout strategies—HLA-I KO (α -chain knockout), TCR KO, TCR–B2M dKO, and
148 MT026 (TCR and HLA-I dKO), with allogeneic PBMCs (NK cell-depleted) or purified
149 NK cells. Knocking out HLA-I effectively prevented rejection by allogeneic T cells
150 (**Figure 1e**). However, these cells still did not evade rejection by NK cells, with effects

151 similar to those observed for the established B2M knockout strategy (**Figure 1f**). These
152 findings highlight the need to integrate HLA-I α -chain knockout with NK-cell
153 suppression strategies or to develop multi-targeted engineering approaches to mitigate
154 residual NK cell-mediated rejection, thereby supporting the development of safer and
155 more effective allogeneic CAR-T therapies.

156

157 ***IL-13Ra2 allogeneic UCAR-T cells potently inhibit glioma growth in vitro and in vivo***

158 To determine whether CRISPR/Cas9-mediated knockout of TCR and HLA-I affects the
159 effector function of IL-13Ra2 allogeneic UCAR-T cells relative to conventional CAR-
160 T cells expressed using a viral system, we first performed *in vitro* cytotoxicity assays
161 against U251 target cells (**Supplementary Fig. 1f; Fig. 2a**). The results indicate that
162 the killing activity of IL-13Ra2 allogeneic UCAR-T cells with HLA-I knockout
163 (MT026) was equivalent to that of allogeneic UCAR-T cells with intact HLA-I.

164 We next investigated optimal E:T ratios by co-culturing glioma organoids expressing a
165 GFP reporter in a time-dependent manner (**Fig. 2b**). Relative GFP fluorescence
166 intensities of glioma organoids were quantified. A visible reduction in GFP fluorescence
167 after >48 h indicated progressive elimination of glioma organoids (**Fig. 2c**). As the E:T
168 ratio increased to 5:1, the cytotoxicity of IL-13Ra2 allogeneic UCAR-T cells was
169 maximized, consistent with the cytotoxicity assays (**Fig. 2a**).

170 Given the pronounced efficacy of IL-13Ra2 allogeneic UCAR-T cells *in vitro*, we
171 further assessed antitumor effects in a patient-derived orthotopic xenograft (PDX)
172 model using female 6-week-old BALB/c-*nu* mice. Ten fully formed organoids (1 mm
173 diameter) were transplanted into the brain. Glioma organoid cells were transduced to
174 express a luciferase reporter, enabling quantification throughout the study by
175 bioluminescence imaging (BLI; **Fig. 2d**).

176 The survival curve of the PDOX model indicated that IL-13R α 2 allogeneic UCAR-T
177 therapy suppressed tumor progression *in vivo* and improved survival, whereas mice in
178 the no-treatment control (NT) group exhibited continuous tumor proliferation, resulting
179 in death from day 30 onward (Fig. 2e). Brain tumor growth was significantly
180 suppressed for 7 days after intratumoral injection of IL-13R α 2 allogeneic UCAR-T
181 cells; however, slight tumor recurrence was observed since 14th day after injection (day
182 29 after model initiation) (Fig. 2f). Quantitative analysis of BLI in PDOX mice was
183 consistent with survival results: the control group showed a substantial increase in
184 bioluminescence, whereas the experimental group exhibited only a minimal increase
185 (Fig. 2g). Taken together, the *in vitro* and *in vivo* data indicate that IL-13R α 2 allogeneic
186 UCAR-T therapy effectively inhibits tumor growth and confers sustained tumor
187 suppression in model animals.

188

189 ***Clinical trial - Patients and treatment overview***

190 The key objective was to assess the clinical feasibility, tolerability, and safety of
191 intrathecal administration of CRISPR-Cas9-edited allogeneic IL-13R α 2 UCAR-T cells
192 for treatment of recurrent high-grade glioma (WHO grades 3 and 4) after standard
193 tumor resection with chemoradiotherapy. The study, which ran from August 2020 to
194 July 2022, faced operational challenges due to COVID-19 restrictions. As a result,
195 enrollment, dose-escalation schedules, and assessment schedules were impacted. Five
196 eligible patients with recurrent IL-13R α 2-overexpressing glioblastoma out of a planned
197 twelve were enrolled and received study treatment and assessments. When visits were
198 missed due to pandemic restrictions, follow-up calls were performed to monitor patient
199 safety and survival status. All patients were followed until death upon the development
200 of disease progression. The derived data were valuable for understanding preliminary

201 safety and therapeutic response to CRISPR-Cas9–edited allogeneic IL-13R α 2 UCAR-
202 T cells delivered intrathecally in a patient context.

203 All five patients were Chinese, with a mean age of 52 years (range, 45–63), and four
204 were women. Four patients had KPS <70, and one had KPS 90; the mean KPS was 60.
205 Four of five had medium IL-13R α 2 expression, and one (MT026-02) had high
206 expression before study entry (**Table 1**). All patients shared the same prognostic genetic
207 profile: IDH-wildtype and MGMT promoter–unmethylated. Each patient received at
208 least one round of conventional therapy, including surgical resection and systemic
209 chemotherapy (temozolomide) and radiation, before study entry.

210 Patients received more than four intrathecal injections of CAR-T cells, totaling 1.0×10^7
211 to 3.0×10^7 cells over 3.4 months of exposure, with the longest course comprising eight
212 injections over up to 7.9 months (MT026-02) before disease progression
213 (**Supplementary Fig. 2**). At the PI's discretion, patient MT026-02 continued with two
214 additional study-drug administrations after concurrent surgical treatment with
215 chemoradiation at progression (**Supplementary Fig. 2b,c**).

216 After disease progression in patient MT026-003, a tumor biopsy was performed, and
217 other investigational targeted cell therapies—EGFR-targeted or B7H3-targeted cells—
218 were administered based on new targets identified by immunohistochemistry
219 (**Supplementary Fig. 2d**).

220

221 *Clinical bioactivity of IL-13R α 2 allogeneic UCAR-T cell administration via an*
222 *intrathecal route*

223 Of five patients, CSF CAR DNA copies were consistently elevated 1 day after each of
224 the first five study-drug administrations, peaked 2–4 days after infusion, and remained
225 detectable between consecutive injections with repeated intrathecal dosing in patient

226 MT026-005. CSF CAR DNA copies reached maximal levels from baseline after the
227 fourth intrathecal injection in patients MT026-004 and MT026-005. (**Fig. 3a, b** and
228 **Supplementary Fig. 3**). No CAR DNA copies were detected in peripheral blood at any
229 time point (data not shown). While the observed high CAR DNA peaks suggest that
230 cell expansion may have occurred following intrathecal injection, we cannot
231 definitively confirm expansion of the cells *in vivo*.

232 Effector cytokines, including TNF α , IFN γ , IL-2, IL-6, IL-8, and IL-10, and
233 chemokines, including CCL2 and CXCL10, increased in CSF after intrathecal delivery
234 of the study drug in patient MT026-005 (**Fig. 3c**). These changes, exemplified by CSF
235 IL-6 elevation, appeared temporally associated with increases in CSF CAR DNA
236 copies, as observed in patients MT026-004 and MT026-005.

237 Peripheral blood IL-6 concentrations were elevated after each CAR-T administration;
238 however, levels were lower than in CSF, with CSF concentrations 79- to 647-fold
239 higher than blood. These data suggest a more localized effector response at tumor
240 proximity (patients MT026-004 and MT026-005), **Fig. 3d**.

241 In Patient MT026-005, the blood lymphocyte count was low at baseline and increased
242 with treatment. In this patient, the blood neutrophil-to-lymphocyte ratio was high at
243 baseline and decreased in response to treatment (**Fig. 3e,f**). These results are consistent
244 with the notion that early NLR reduction is significantly associated with better
245 prognosis in mCRC patients treated with immunotherapy [26].

246

247 ***Safety of repeated exposure of IL-13Ra2 allogeneic UCAR-T cell administration via***
248 ***an intrathecal route***

249 During the study, study drug-related adverse events included fever (4/5, 80 %), hypoxia
250 (2/5, 40 %), vomiting (2/5, 40 %), and headache (1/5, 20 %) (**Table 2**). These AEs were

251 grade 1 or 2 and resolved or stabilized spontaneously or with optimal management.
252 Reported CSF laboratory abnormalities were increased interleukin-6 (5/5, 100 %),
253 increased total protein (4/5, 80 %), and increased lactate dehydrogenase (3/5, 60 %).
254 Serum laboratory abnormalities included elevated IL-6 in two of five patients (2/5,
255 40 %) and elevated C-reactive protein in three of five patients (3/5, 60 %). These
256 elevated cytokine and proinflammatory markers were most likely part of downstream
257 signaling stimulated by CAR-T immunotherapy delivered into the CSF space and
258 circulating in the blood, as described above.

259 No grade ≥ 3 AEs, SAEs, immune effector cell–associated neurotoxicity syndrome
260 (ICANS), GvHD, or infections were reported during the study. Only Grade 1 AEs were
261 observed, including myelosuppression (decreased lymphocytes and leukocytes),
262 leukocytosis, and Grade 1 cytokine release syndrome (CRS) manifesting as fever
263 (Table 3). In summary, repetitive dosing of up to 8 infusions of IL-13Ra2-specific
264 CAR-T cell clones, with doses ranging from 1.0×10^7 to 3.0×10^7 cells administered into
265 the CSF space via an intrathecal route, exhibited an acceptable safety profile with
266 limited, transient, low-grade adverse events.

267

268 ***Evidence of preliminary therapeutic benefit of IL-13Ra2 allogeneic UCAR-T cell
269 intrathecal administration in a patient context***

270 Although therapeutic benefit could not be established in this small cohort, we report
271 individual patient–level data on the preliminary efficacy of this CRISPR-Cas9–edited
272 allogeneic IL-13Ra2–specific UCAR-T product administered intrathecally in
273 refractory high-grade glioma.

274 Antitumor effect was assessed using the Immunotherapy Response Assessment in
275 Neuro-Oncology (iRANO) criteria. All five patients showed a decrease in tumor size

276 after treatment (**Fig. 4a–e**; **Supplementary Fig. 4**). Among the five patients, the
277 objective response rate (ORR) was 80 % (**Fig. 4d,f; Table 1**), comprising one complete
278 response, three partial responses, and one case of stable disease (**Fig. 4f**). The median
279 duration of response was 3.8 months, with a maximum of 7.4 months (**Fig. 4f ; Table**
280 **3**). Recognizing the limitations of cross-study comparisons, the 80% overall response
281 observed with MT026 appears numerically higher than reported rates with
282 bevacizumab, 25.9 % (95 % CI, 17.0 %, 36.1 %) and 19.6% (95 % CI, 10.9 %, 31.3 %)
283 in two studies [27]. An exceptionally high response rate (4/5) was observed in this
284 difficult-to-treat population (**Table 4**).

285 Patients MT026-001 to MT026-005 survived 5.3, 16.0, 0.9, 3.2, and 7.3 months,
286 respectively, after the first MT026 infusion, with a mean OS of 8.3 months (95 % CI,
287 6.7-9.8), a maximum survival of 17.2 months, and a 12-month OS rate of 20.0% (95 %
288 CI, 3.5-100 %). When survival was calculated from the time of recurrence, the same
289 patients survived 12.8, 33.2, 9.2, 13.7, and 13.1 months, respectively, yielding a median
290 overall survival of 13.1 months (95 % CI, 12.6-13.6) and a 12-month overall survival
291 rate of 80% (95 % CI, 51.6-100 %). The longest survival was 33.2 months for Patient
292 MT026-002 (**Table 1**). Survival in these high-grade patients with glioma appeared
293 numerically better than the expected poor median overall survival of approximately 6
294 to 8 months following recurrence⁴, although comparisons across studies were limited.
295 Mean progression-free survival was 5.6 months (95 % CI: 3.1-8.2), with a maximum
296 of 7.9 months, and the 6-month progression-free survival rate was 40.0 % (95 % CI:
297 11.8-76.9 %). Two of the five patients (MT026-002 and MT026-003) subsequently
298 received additional investigational CAR-T cell therapies as part of subsequent
299 treatment, as indicated in Figure 4c. Patient MT026-002 received two administrations
300 of B7H3 targeted CAR-T cells and one administration of HER2 targeted CAR-T cells,

301 whereas Patient MT026-003 received one administration each of B7H3 and EGFR
302 targeted CAR-T cells.

303 In summary, this study of five subjects with recurrent high-grade glioma demonstrated
304 the feasibility of treating these subjects with engineered allogeneic CAR-T cells via
305 intrathecal delivery to tumor sites. The absence of therapy-related serious adverse
306 events and the potential clinical benefit warrant further investigation.

307

308 **Discussion**

309 Recent studies have investigated CAR T cell therapies for recurrent glioblastoma and
310 other high-grade gliomas, reporting both promising signals and ongoing challenges.
311 Choi et al. (NEJM, 2024) reported rapid, transient tumor regression using CARv3-
312 TEAM-E cells targeting EGFRvIII and wild-type EGFR via intraventricular infusion
313 [28]. Bagley et al. (Nat Med, 2024) evaluated intrathecally delivered bivalent CAR T
314 cells targeting EGFR and IL-13R α 2, demonstrating preliminary safety and bioactivity
315 with early radiographic changes but no confirmed objective responses [29]. Brown et
316 al. (Nat Med, 2024) conducted a phase 1 trial of locoregional IL-13R α 2-targeted CAR
317 T cells in 65 patients, showing acceptable safety and clinical activity, with stable disease
318 or better in 50% of patients but limited median overall survival [30]. This dual-editing
319 strategy in MT026 eliminates TCR-mediated GvHD and reduces HvGR, providing a
320 potential off-the-shelf therapeutic option (Fig. 5). Although these cells, similar to those
321 generated by the existing B2M knockout strategy, still could not evade rejection by NK
322 cells, this approach demonstrated antitumor activity with reduced alloreactivity in both
323 *in vitro* and *in vivo* tumor mouse models via multiplex CRISPR technology. Consistent
324 with the preclinical data, clinical data from this first-in-human, single-center, open-
325 label IIT validated antitumor activity in the study population.

326 Despite the advent of bevacizumab as a treatment option, recurrent glioblastoma
327 remains a largely unmet medical need, highlighting the need for novel and effective
328 therapies. Among emerging therapeutic strategies, CAR-T cells offer potential options
329 for patients refractory to standard therapy. To date, two clinical studies investigating
330 autologous IL-13Ra2-specific CAR-T cells suggest that IL-13Ra2-specific CAR-T
331 cells may be a beneficial therapeutic approach for recurrent glioblastoma, and the
332 intrathecal route has been broadly applied in the clinic because of reduced peripheral
333 organ biodistribution and biased delivery to the brain [27]. However, the time-
334 consuming, complex manufacturing process for autologous CAR-T cells has limited
335 their broader application in candidates for T-cell immunotherapy [9, 31].

336 The study design incorporated the following features to overcome barriers and improve
337 patient benefit: (1) use of "off-the-shelf" allogeneic CAR-T cells to avoid long
338 generation time and to circumvent failed autologous T-cell generation from patient
339 donors with secondary T-cell exhaustion; 2) use of the intrathecal route via lumbar
340 puncture instead of intracavity injection to allow exposure of CAR-T cells to newly
341 seeding lesions, given that multifocal gliomas account for 17.2% of all gliomas [32];
342 (3) use of intrathecal delivery via lumbar puncture instead of the intraventricular route
343 to improve ease of administration, as drug distribution in CSF via intraventricular or
344 intrathecal routes is similar 4-6 h after administration[33]; 4) use of monthly rather than
345 weekly dosing to reduce patient burden in clinic settings; and (5) elimination of
346 lymphodepletion. Preconditioning with lymphodepleting agents may create a
347 "favorable" environment for expansion and survival of CAR-T cells in the body by
348 eliminating regulatory T cells; however, this step is used primarily in intravenous CAR-
349 T cell therapy. There is still controversy over whether CAR-T will produce different
350 effects after lymphodepleting chemotherapy in solid tumors. The pre-conditioning with

351 lymphodepleting chemotherapy is not necessary for a local route of administration; it
352 remains uncertain whether lymphodepleting chemotherapy is necessary [34, 35].

353 The clinical data showed favorable tolerability and safety profiles, with no grade 3 or
354 higher adverse events, no typical or severe cytokine release syndrome, and no severe
355 neurotoxicity. These findings are consistent with other clinical studies involving IL-
356 13R α 2-specific CAR-T cells [9,31] using local product delivery. A plausible
357 explanation is that lower tumor burden and lack of prior lymphodepletion contribute to
358 the absence of cytokine release syndrome and neurotoxicity, even when cell doses in
359 these studies were comparable to those administered to patients with B-cell
360 malignancies [36–38]. However, another study reported more severe adverse events at
361 higher cell doses [31], suggesting a dose-dependent safety pattern. In published studies
362 of GD2 CAR-T cells in patients with H3K27M-mutated diffuse midline gliomas,
363 neurotoxicity was observed in patients treated with ICV. No significant neurotoxicity
364 was observed in this study, and blood IL-6 levels were significantly lower than those in
365 CSF, possibly related to the CAR-T cell construct and the total number of cells injected
366 into CSF [39], suggesting that intrathecal administration via lumbar puncture may limit
367 systemic effects.

368 Notably, MT026 did not result in any adverse events related to graft-versus-host disease
369 [40], which supports the approach of constructing allogeneic universal CAR-T cells by
370 knocking out T-cell receptor α chains with CRISPR/Cas9 technology to eliminate this
371 specific toxicity.

372 The study population was more advanced, with worse disease status (i.e., lower KPS)
373 and faster disease progression as indicated by baseline prognostic markers (MGMT,
374 IDH1/IDH2), compared with participants in other pivotal studies. Baseline
375 characteristics included KPS ≥ 40 with a mean of 60, whereas the published cohort

376 required KPS ≥ 70 [27]. In addition, methylated MGMT status is the strongest predictor
377 of prolonged survival in GBM, and gliomas with mutated IDH1 or IDH2 have improved
378 prognosis compared with gliomas with wild-type IDH1/IDH2 [41]. All five patients in
379 this study had unmethylated MGMT and wild-type IDH1/2, whereas published cohorts
380 included both wild-type and mutant IDH1/2 and a mix of methylated and unmethylated
381 MGMT promoters (**Table 5**) [41-46]. It is encouraging that the overall response rate of
382 MT026 was numerically higher than that reported in bevacizumab studies that enrolled
383 populations with higher KPS (90–100 for 45 % of patients and 70–80 for 55 % of
384 patients in one study; 90-100 for 68 % of patients in another), although other differences
385 between MT026 and bevacizumab study designs limit direct comparison.

386 Several published studies have shown that long-term remissions of hematologic
387 malignancies are associated with expansion and sustained persistence of CAR-T cells
388 [47]. Based on preliminary data, we hypothesize that CAR-T cell expansion and
389 persistence in brain tumor areas, delivered via lumbar infusion, may have contributed
390 to the immune response and the remissions observed in patients with glioma treated
391 with MT026 CAR-T cells.

392 MRI does not necessarily distinguish between tumor, edema, and radiation necrosis.
393 We expect that allogeneic UCAR-T cells will continuously infiltrate, proliferate, and
394 elicit inflammation within tumor tissue [40,48]. A study of CAR-T cell therapy for
395 H3K27M-mutated diffuse midline gliomas demonstrated that pseudo-progression may
396 occur within days after therapy and lasts only several days [39]. A more intensive
397 radiographic assessment schedule should be implemented to further characterize
398 pseudo-progression related to MT026.

399 As previously reported, when survival was calculated from the first MT026 infusion,
400 the OS of the five enrolled patients ranged from 0.9 to 16.0 months, with a 12-month

401 OS rate of 20.0 % (95 % CI, 3.5-100 %). When calculated from the time of recurrence,
402 the same patients survived 9.2 to 33.2 months, with a 12-month overall survival rate of
403 80 % (95 % CI, 51.6-100 %). Although these values appear numerically superior to the
404 epidemiologically reported median OS of 6-8 months for recurrent high-grade glioma,
405 interpretation of the potential survival benefit attributable to MT026 is limited by
406 several factors. First, most observed responses were short-lived: Patient MT026-003
407 exhibited loss of IL-13Ra2 expression after re-biopsy, suggesting immune escape due
408 to target loss; Patient MT026-004 discontinued MT026 after only four infusions for
409 personal reasons; and Patient MT026-005 experienced highly aggressive tumor growth,
410 with progression occurring within 33 days post-surgery, likely reflecting extreme tumor
411 kinetics and suboptimal dosing frequency. Second, the limited sample size and the fact
412 that two of the five patients received additional investigational UCAR-T therapies
413 targeting other antigens further confound interpretation. Despite these limitations, the
414 clinical data provide preliminary efficacy signals, including tumor responses and
415 potential survival benefit, supporting the need for larger-scale, randomized controlled
416 trials to more definitively determine the therapeutic impact of MT026 in this patient
417 population.

418 In summary, this study report an approach using allogeneic IL-13Ra2-specific CAR-T
419 cells designed to enhance the persistence of IL-13Ra2-specific allogeneic CAR-T cells,
420 with a tolerable safety profile and potential clinical benefits in recurrent high-grade
421 glioma. These findings support further clinical investigation in this patient population.
422 Moving forward, we will incorporate a prespecified translational framework into future
423 cohorts to strengthen mechanistic understanding and enhance platform generalizability.
424 Specifically, we plan to perform serial CSF-based TCR sequencing and immune
425 phenotyping to dynamically monitor CAR-T cell clonal expansion and persistence,

426 utilize single-cell cytokine profiling to comprehensively characterize immune
427 activation, and include NK-activity readouts to evaluate innate immune responses.
428 Moreover, considering that allogeneic CAR-T cells remain vulnerable to NK cell-
429 mediated clearance, we will explore mitigation strategies such as HLA-E
430 overexpression to engage inhibitory NK receptors, CIITA knockout to reduce HLA
431 class II expression, and CD47 engineering to deliver “don’t eat me” signals. Integration
432 of these translational approaches will provide key insights into mechanisms of
433 therapeutic resistance, optimize CAR-T cell persistence, and facilitate broader
434 applicability of this platform-based strategy.

435

436 **Methods**

437 ***Production of lentiviral vectors***

438 HEK 293T cells (ATCC, # CRL-3216) were cultured in 10-cm dishes and transfected
439 at a density of 6×10^5 cells/mL. Transfection used PEI complexes containing VSV-G
440 (3.5 μ g), GagPol (5.5 μ g), Rev (2.5 μ g), and the transfer vector MK005-A (10 μ g;
441 encoding the CARs). Lentiviral supernatants were collected 48 h after transfection,
442 passed through a 0.45 μ m filter, and concentrated by centrifugation for 2 h at 50,000 g.
443 Lentiviral vector titers (TU/mL) were determined by serial dilution, and the percentage
444 of CAR-positive cells was measured by flow cytometry 7 days post-transduction.

445 ***Manufacturing of cell products***

446 The IL-13R α 2 CAR sequence (WO/2014/072888, Pfizer INC.) was cloned into the
447 lentiviral vector backbone. T cells collected from healthy donors were enriched by
448 magnetic separation using anti-CD4 and anti-CD8 microbeads (Miltenyi Biotec), and
449 activated with T Cell TransAct (Miltenyi Biotec). At 24 h after activation, lentivirus
450 was mixed with T cells at a final MOI of 3 in 6-well round-bottom plates. For each well,

451 5×10^6 T cells were combined with medium containing lentivirus (1×10^9 TU/mL) in
452 15 μ L and then spinfected at $800 \times g$ for 60 min. Cells from the same condition were
453 pooled and seeded at 5×10^5 cells/mL in culture flasks. Two days post-transduction, cells
454 were collected and pelleted for nucleofection of Cas9 ribonucleoproteins (RNPs) to
455 generate TCR and HLA-I knockouts. sgRNA for the *HLA-I* α chain: 5'-
456 CTGACCATGAAGCCACCCTG-3'; sgRNA for *TRAC*: 5-
457 AGAGTCTCTCAGCTGGTACA-3'; sgRNA for B2M: 5-
458 GAGTAGCGCGAGCACAGCTA-3'. RNPs for each target locus were complexed
459 separately at a 2.5:1 sgRNA (GenScript Biotech): SpCas9 (Thermo) ratio. The two
460 RNPs were then combined to 42 pmol *TRAC* RNP and 42 pmol *HLA-I* RNP per million
461 cells. The RNP mixture was diluted in P3 solution (Lonza) and mixed with the cell
462 pellet, then nucleofected using the EO115 program (Lonza). Nucleofected cells were
463 seeded at 1×10^6 cells/ mL. Magnetic separation using anti-CD3 microbeads (Miltenyi
464 Biotec) was performed to remove CD3+ cells and improve the purity of allogeneic
465 universal CAR-T cells. T cells were cultured in X-VIVO 15 medium (Lonza)
466 supplemented with 5% CTS Immune Cell Serum Replacement (Gibco), recombinant
467 human IL-2 (200 U/mL), IL-7 (10 ng/mL), and IL-15 (5 ng/mL) for 14 days. Cell
468 products were stored in cryoprotectant after harvest.

469 ***Off-target analysis:***

470 To assess CRISPR-Cas9 off-target activity, multiple sequencing methods were
471 employed. In AID-seq, genomic DNA from unedited T cells was fragmented, ligated to
472 hairpin adapters, and digested with exonucleases to reduce false positives. Cleavage by
473 Cas9 ribonucleoprotein exposed ends for biotinylated adapter ligation, followed by
474 streptavidin enrichment, nested PCR, and alignment to identify on- and off-target sites.
475 GUIDE-seq and iGUIDE-seq utilized dsODN tags integrated via NHEJ to mark

476 cleavage sites in living T cells. iGUIDE-seq employed a longer dsODN for improved
477 precision. Tagged DNA was fragmented, adapter-ligated, and PCR-amplified before
478 sequencing and alignment. PEM-seq involved shearing DNA, PCR extension with
479 biotinylated primers, and dual barcoding before high-throughput sequencing and
480 analysis via PEM-Q. For editing efficiency, amplicon sequencing of target regions was
481 performed, followed by CRISPResso analysis for quality control, alignment, and indel
482 characterization. All methods enabled comprehensive profiling of CRISPR-induced on-
483 and off-target edits.

484 ***Primary natural killer cell (NK Cell) rejection assay:***

485 Isolate natural killer cells (NK cells) from peripheral blood mononuclear cells (PBMCs)
486 by positive selection with CD56 magnetic beads, label them with Far Red fluorescent
487 dye (Thermo Fisher Scientific, Cat# C34572), co-culture them with CTV-labeled
488 UCAR-T cells or K562 cells (Cat# 1101HUM-PUMC000039) which were purchased
489 from the Cell Bank of the Chinese Academy of Science (Shanghai, China) at ratios of
490 2:1, and assess UCAR-T cell survival at 48 h. PBMCs used for NK cell isolation were
491 obtained from healthy donors who provided written informed consent, and the
492 procedure was approved by the Medical Ethics Committee of Ningbo University
493 Affiliated People's Hospital (approval number: 2024-013).

494 ***Graft-versus-host reaction (GVHR) assay:***

495 Label universal chimeric antigen receptor T cells (UCAR-T cells) from different groups
496 with Carboxyfluorescein Diacetate Succinimidyl Ester (CTV) (Thermo Fisher
497 Scientific, Cat# C34557), co-culture them with allogeneic peripheral blood
498 mononuclear cells (PBMCs) treated with mitomycin at a ratio of 2:1 for 5 days (120 h),
499 and assess the fluorescence shift of CTV in UCAR-T cells relative to the group
500 containing only UCAR-T cells (Only group).

501 ***Mixed lymphocyte reaction (MLR) assay:***

502 After isolating natural killer cells (NK cells) from PBMCs using CD56 magnetic beads
503 (Miltenyi Biotec, Cat# 130-050-401) , co-culture them with CTV-labeled UCAR-T
504 cells at a ratio of 10:1 for 12 days. Replace the culture medium every 3 days, stain with
505 CD3 and a Fixable Viability Dye by flow cytometry, and analyze longitudinal changes
506 in the numbers of UCAR-T cells and allogeneic T cells.

507 ***In vitro CAR T Cell Killing assay***

508 UCAR-T cells and control cells (Mock-T) were co-cultured at different ratios with the
509 U251 cell lines (Cat# BFN608006387) which were purchased from the Cell Bank of
510 the Chinese Academy of Science (Shanghai, China) for 24 hours. The U251 cell lines
511 were pre-labeled with CellTrace™ Violet, and post-co-culture cell viability was
512 assessed by PI staining. Flow cytometry was performed to quantify dead target cells,
513 and the percentages of specific CAR-T killing were calculated using the formula: (Dead
514 target cells% -Spontaneous dead target cells %) / (100- Spontaneous dead target cells
515 %) x 100.

516 ***Co-culture of CAR-T cells with glioma organoids***

517 All patient-derived organoids used in this experiment were obtained with written
518 informed consent from the donors, and the use of these specimens was approved by the
519 Medical Ethics Committee of the Fourth Affiliated Hospital of Soochow University
520 (Dushu Lake Hospital) (approval number: 190009). According to the neural tissue
521 dissociation kit instructions, dissociate approximately five organoids measuring 1-1.5
522 mm in diameter. Perform manual cell counts in triplicate to determine the average cell
523 number within the 1-1.5 mm range. Pre-recover CAR-T cells and assess viability by
524 trypan blue exclusion. Transfer individual organoids into separate wells of a 96-well
525 plate and add CAR-T cells at the desired effector-to-target ratios. Bring the volume to

526 250 μ L with T-cell culture medium. Incubate at 37 °C, 5 % CO₂, and 90 % relative
527 humidity, and co-culture on a shaker at 120 rpm. At specified time points, collect
528 supernatant for cytokine analysis, perform immunofluorescence imaging of organoids,
529 or fix organoids for immunohistochemical analysis. The glioma organoid samples are
530 preserved at the Fourth Affiliated Hospital of Soochow University for further analyses.
531 Requests for access to these samples should be directed to the corresponding author.

532 ***Patient-derived orthotopic xenograft (PDOX) models***

533 All animal experiments complied with relevant ethical regulations and were approved
534 by the Animal Ethics Committee of the Fourth Affiliated Hospital of Soochow
535 University (Dushu Lake Hospital) (approval number: 190009). Female BALB/c-nu
536 nude mice (6 weeks old) were used in this study. Mice were housed under standard
537 conditions with a 12-hour light/dark cycle, an ambient temperature of 22 ± 2 °C, and
538 relative humidity of 50 ± 10 %. The choice of sex was based on experimental
539 consistency and previous literature showing comparable tumor growth kinetics in
540 female nude mice; therefore, sex was not considered as a biological variable in data
541 analysis.

542 We ground the tips of the spinal needles and sterilized them at high temperature in
543 advance. Anesthetize the mice with isoflurane and secure each mouse's head in a
544 stereotaxic frame. Maintain continuous anesthesia via a face mask. Using long forceps,
545 pick up organoids individually and load them into the proximal end of the lumbar
546 puncture needle. Fix the needle in the syringe holder of the stereotaxic frame. Disinfect
547 the scalp with 75 % ethanol. Make a longitudinal incision of approximately 0.7 cm
548 slightly posterior to the line connecting the eyes. Using a 2.0 mm electric grinder bit,
549 create a small hole 2 mm posterior to the right side of the fontanelle. With the
550 stereotaxic instrument, position the needle tip in the hole, ensuring contact with the

551 brain surface. Slowly lower the needle by 2.5 mm and wait for 2 min. Retract the needle
552 by 0.5 mm and slowly inject the organoids. Leave the needle in place for 2 min, then
553 remove it slowly. Close the cranial window with bone wax and suture the skin.
554 After tumor formation, immobilize the mice and sterilize the scalp as described above.
555 Lower a Hamilton syringe 2.5 mm beneath the skull surface and inject 5 μ L of
556 concentrated CAR-T cells (total CAR-T cell number five times the initially implanted
557 organoid cell count). Withdraw the Hamilton syringe after 2 min and suture the skin. In
558 vivo bioluminescence imaging was performed at regular intervals to monitor tumor
559 progression and therapeutic response. Euthanasia was performed when predefined
560 humane endpoints were reached, including: >20% body weight loss compared with
561 baseline, persistent weight loss >15% over 48 hours, severe neurological deficits (e.g.,
562 seizures, circling, loss of righting reflex, or inability to ambulate), marked reduction in
563 activity or inability to access food and water, severe distress or pain unrelieved by
564 analgesics, or rapid tumor-associated neurological deterioration. Mice meeting any of
565 these criteria were euthanized using CO₂ inhalation followed by cervical dislocation in
566 accordance with institutional ethical regulations.

567 ***Flow Cytometry Analysis***

568 For flow cytometry, the antibodies used included HLA-ABC-APC (clone W6/32,
569 Thermo Fisher Scientific, Cat# 17-9986-42), TCR-APC (clone IP26, Thermo Fisher
570 Scientific, Cat# 17-9986-42), CD137-BV421 (clone 4B4-1, BD Biosciences, Cat#
571 564091), CD69-FITC (clone EN50, BioLegend, Cat# 310904), IL-13Ra2-PE (clone 47,
572 BioLegend, Cat# 360306), CD62L-PerCP-eFluor710 (clone DREG-56, Thermo Fisher
573 Scientific, Cat# 46-0629-42), and CD45RO-FITC (clone UCHL1, BioLegend, Cat#
574 304242). Detailed information of all antibodies, including clones, manufacturers and
575 catalog numbers, and dilutions ratio were summarized in **Supplemental Table 5**. For

576 flow cytometry analysis, cells were sampled and washed with FACS buffer (DPBS with
577 0.5 % BSA), incubated with antibodies in FACS buffer on ice in darkness for 30 min,
578 washed again with FACS buffer twice. Samples were acquired on a CytoFLEX flow
579 cytometer (Beckman Coulter Life Sciences) and analyzed using FlowJo software
580 (v10.1, Tree Star).

581 ***Healthy donor***

582 Donors were initially healthy volunteers who were screened using a questionnaire
583 addressing risk factors for transmissible and hematologic diseases. Donors were
584 required to be <30 years of age, have a body mass index <30 kg/m², test negative for
585 cytomegalovirus, and be homozygous for HLA-A*02. Donor screening and eligibility
586 were determined per 21 Code of Federal Regulations 1271 criteria. Donors were
587 screened for hepatitis B, hepatitis C, human immunodeficiency virus 1/2, human T-
588 lymphotropic virus I/II, cytomegalovirus, syphilis, West Nile virus, Chagas
589 (Trypanosoma cruzi), human herpesvirus 6/7/8, BK virus, Epstein–Barr virus, and
590 human parvovirus B19. ABO and Rh typing were performed for all donors. HLA
591 confirmatory typing was completed during screening. Additional information on
592 healthy donors is provided in the Methods in the **Supplementary Table 1**.

593 ***Patients***

594 This study complied with all relevant ethical regulations and was approved by the
595 Ethics Committee of the First Affiliated Hospital of Soochow University (approval
596 number: 2020001). The study was conducted in accordance with the principles of the
597 Declaration of Helsinki. All patients enrolled met the ethical requirements for tumor
598 burden, with actual tumor volume not exceeding the maximum limit approved by the
599 ethics committee, defined as $\leq 5 \text{ cm} \times 4 \text{ cm} \times 3 \text{ cm}$ (approximately 30 mL) on MRI.
600 We enrolled adults with histologically or cytologically confirmed recurrent

601 glioblastoma with IL-13Ra2 antigen expression $\geq 50\%$ in tumor tissue. Patients were
602 required to have received prior standard-of-care treatment for glioblastoma and to have
603 relapsed with measurable tumor lesions according to the Immunotherapy Response
604 Assessment in Neuro-Oncology (iRANO) criteria of the Response Assessment in
605 Neuro-Oncology Working Group, and to have a Karnofsky Performance Score (KPS)
606 ≥ 40 (on a 100-point scale, with lower numbers indicating greater disability). This study
607 was preregistered in the Chinese Clinical Trial Registry (ChiCTR2000028801), with
608 the first posting date on January 4 2020 and the study initiation date on July 1 2020.
609 The last patient was enrolled on January 14, 2022. The study registration can be
610 accessed at <https://www.chictr.org.cn/showproj.html?proj=47867>. The originally
611 planned enrollment of 12 patients was reduced to 5 due to delays caused by the COVID-
612 19 pandemic. The study protocol and endpoints reported in this manuscript remain
613 consistent with the preregistered version. Consent to publish clinical information
614 potentially identifying individual participants was obtained from all enrolled patients.

615 ***Detection of IL-13Ra2 Expression in Tumor Tissues***

616 IL-13Ra2 expression in tumor tissues was assessed by immunohistochemistry (IHC)
617 based on the principle of specific antigen–antibody binding. Formalin-fixed, paraffin-
618 embedded tumor sections were incubated with a rabbit anti-human IL-13Ra2/CD213a2
619 monoclonal antibody (clone E7U7B, Cat. #85677, Cell Signaling Technology, USA),
620 followed by horseradish peroxidase (HRP)-conjugated secondary antibody (Cat. #7074,
621 CST). Visualization was achieved using 3,3'-diaminobenzidine (DAB; Cat.#8059, CST)
622 as the chromogenic substrate, and sections were counterstained with hematoxylin. IL-
623 13Ra2 antigen–positive cells exhibited membranous or cytoplasmic staining ranging
624 from light yellow to dark brown. For scoring, tumor samples were classified as IL-
625 13Ra2-positive when $\geq 50\%$ of tumor cells displayed staining, consistent with the

626 study's enrollment criteria. Expression levels were further categorized as follows:
627 medium expression was defined as 50–69 % of tumor cells with weak-to-moderate
628 staining, whereas high expression was defined as ≥ 70 % of tumor cells with moderate-
629 to-strong staining.

630 ***Study design and treatment***

631 In this single-center, open-label, single-arm, exploratory trial, patients received MT026,
632 an IL-13R α 2-specific allogeneic universal CAR-T cell preparation (IL-13R α 2
633 allogeneic UCAR-T cells; target dose, 2.5×10^7 cells, actual doses, $1.0\text{--}3.0 \times 10^7$ cells),
634 administered by intrathecal lumbar puncture once monthly until disease progression,
635 unacceptable toxicity, withdrawal of consent, death, loss to follow-up, or
636 discontinuation for the benefit of patients at the discretion of the investigator. Dose
637 selection for each patient was guided by clinical tolerance and safety considerations: if
638 a patient developed fever up to 39 °C (corresponding to Grade 2 CRS), dose escalation
639 was halted. For example, Patient MT026-002 had already achieved a complete response
640 after treatment, and further dose escalation was not pursued to minimize risk of severe
641 complications such as cerebral edema. Accordingly, the principal investigator chose to
642 continue treatment at intermediate doses that had demonstrated both safety and early
643 signs of efficacy. Dose adjustment was permitted in the event of severe toxic effects or
644 inadequate therapeutic effect (**Supplementary Fig. 2**).

645 ***Assessment***

646 Efficacy was assessed by brain magnetic resonance imaging (MRI; gadolinium-
647 enhanced T1 and T2/FLAIR sequences), as well as new lesions, corticosteroid use, and
648 clinical status according to iRANO criteria for CNS tumors. MRI was performed at
649 baseline and then monthly until the end of treatment, and images were evaluated by
650 radiologists. Two radiologists (Y.Z. and A.J.D.; 20 and 6 years of experience in

651 neuroradiology, respectively) independently interpreted the images and conducted two-
652 dimensional tumor measurements while blinded to clinical outcomes. Data from Y.Z.
653 were used for analysis, and data from A.J.D. were used to test repeatability. The
654 intraclass correlation coefficient (ICC) for tumor size between the two radiologists was
655 0.916 (95 % CI: 0.819–0.963, $P < 0.001$). Disease progression and survival status were
656 assessed and recorded every 3 months. Baseline IL-13Ra2 expression in archival or
657 newly obtained formalin-fixed tumor samples was assessed at a local laboratory using
658 an investigational immunohistochemistry assay developed by T-MAXIMUM.

659 Adverse events were monitored during treatment and for 30 days after the end of
660 treatment (90 days for serious adverse events). Events of interest specific to allogeneic
661 universal CAR-T cells included cytokine release syndrome, immune effector cell-
662 associated neurotoxicity syndrome, and graft-versus-host disease.

663 CAR DNA copies in CSF before and 1 day after each administration were quantified
664 using an investigational assay developed by T-MAXIMUM. Routine CSF and blood
665 tests and genetic testing were performed at a local laboratory. Cerebrospinal fluid and
666 blood IL-6 concentrations were assessed by another local laboratory before and 1 day
667 after each administration.

668 ***End points***

669 The primary endpoint was the occurrence and severity of adverse events among all
670 patients who received at least one dose of MT026. Secondary end points included
671 overall survival, progression-free survival, objective response rate, duration of response,
672 disease control rate, and pharmacokinetic parameters. Exploratory endpoints were PK
673 characteristics (CAR DNA copies), changes in pharmacodynamic (PD) parameters
674 (cytokines, lymphocyte count, and neutrophil-to-lymphocyte ratio), and relationships
675 between demographic stratification variables (sex, KPS, IL-13Ra2 antigen expression

676 level, IDH1/2 mutation, and MGMT promoter methylation) and response. Adverse
677 events were graded according to the National Cancer Institute Common Terminology
678 Criteria for Adverse Events, version 5.0 (NCI CTCAE 5.0). All efficacy endpoints were
679 evaluated according to iRANO criteria for CNS tumors.

680 ***Statistical analysis***

681 A sample size of 12 patients was predicated on the assumption that it would be sufficient
682 to assess the initial acute and severe toxicity of MT026 at the tested dose in humans.
683 Adverse event frequency and severity were tabulated by preferred terms and
684 summarized using descriptive statistics. Rates of objective response, progression-free
685 survival, and overall survival were summarized as percentages and estimated using
686 Kaplan–Meier methods, with curves presented. Overall survival, progression-free
687 survival, duration of response, and time to response were summarized as medians in
688 months. Ninety-five percent confidence intervals for these parameters were calculated
689 using the Clopper–Pearson exact method.

690 ***Data gathered and stored***

691 During data collection, respondents were clearly informed of the study purpose and
692 data confidentiality, and patient information was collected only after consent was
693 obtained. During data analysis, researchers evaluated the treatment process, while MRI
694 images and laboratory test data were processed by specialists. These procedures were
695 implemented to ensure scientific rigor and data accuracy.

696 ***Study oversight***

697 This investigator-initiated study was approved by the institutional review boards of The
698 First Affiliated Hospital of Soochow University and The Fourth Affiliated Hospital of
699 Soochow University. All patients provided written informed consent before enrollment,
700 in accordance with the principles of the Declaration of Helsinki. All healthy donors

701 provided written informed consent before T-cell donation. The authors vouch for the
702 completeness and accuracy of the data and the fidelity of the study to the protocol.

703 **Sex and gender considerations**

704 This study enrolled both male and female patients with recurrent glioblastoma. The
705 inclusion criteria were based solely on clinical and molecular characteristics, regardless
706 of sex or gender. Given the small sample size (n=5), no sex- or gender-based statistical
707 analyses were performed, as the study was not powered to detect sex- or gender-related
708 differences. Sex of participants was determined based on self-report during enrollment.

709

710 **Data Availability Statement**

711 The off-target detection datasets—comprising GUIDE-seq, PEM-seq, AID-seq, and
712 amplicon sequencing—have been deposited in the Genome Sequence Archive in the
713 National Genomics Data Center, China National Center for Bioinformation, under
714 accession code HRA015321 [<https://ngdc.cncb.ac.cn/gsa-human/browse/HRA015321>].
715 To protect donor privacy concerning HLA genetic sequences, these data are under
716 controlled access for two years following publication. During this two-year controlled-
717 access period, qualified researchers may request access through the GSA controlled-
718 access system or by contacting the corresponding author, Yulun Huang (Y.H.), for
719 legitimate scientific purposes. Additionally, since the sequencing primers used in the
720 data analysis methods implicate donor HLA privacy, all inquiries concerning data
721 analysis methods must be addressed directly to the corresponding author. A copy of the
722 study protocol is available in the Supplementary Information file. Individual de-
723 identified participant data, including clinical information, imaging data, and treatment
724 responses, are provided in the manuscript and/or the Supplementary Information.
725 Additional de-identified participant-level data may be made available for academic,

726 non-commercial research purposes upon reasonable request to the corresponding author
727 Yulun Huang (Y.H.), subject to institutional approvals and a data-sharing agreement.
728 All other data supporting the findings of this study are available in the article, its
729 supplementary files and source data and/or from the corresponding author upon
730 reasonable request. Source data are provided with this paper.

731

732 **Reference**

- 733 1. Ostrom, Q.T., et al., CBTRUS Statistical Report: Primary Brain and
734 Other Central Nervous System Tumors Diagnosed in the United States in 2011-
735 2015. *Neuro Oncol*, 2018. 20(suppl_4): p. iv1-iv86.
- 736 2. Horbinski, C., et al., NCCN Guidelines(R) Insights: Central Nervous
737 System Cancers, Version 2.2022. *J Natl Compr Canc Netw*, 2023. 21(1): p. 12-
738 20.
- 739 3. Stupp, R., et al., Effect of Tumor-Treating Fields Plus Maintenance
740 Temozolomide vs Maintenance Temozolomide Alone on Survival in Patients
741 With Glioblastoma: A Randomized Clinical Trial. *JAMA*, 2017. 318(23): p.
742 2306-2316.
- 743 4. Walbert, T. and T. Mikkelsen, Recurrent high-grade glioma: a diagnostic
744 and therapeutic challenge. *Expert Rev Neurother*, 2011. 11(4): p. 509-18.
- 745 5. Bagley, S.J., et al., CAR T-cell therapy for glioblastoma: recent clinical
746 advances and future challenges. *Neuro Oncol*, 2018. 20(11): p. 1429-1438.
- 747 6. Lin, Y.J., L.A. Mashouf, and M. Lim, CAR T Cell Therapy in Primary
748 Brain Tumors: Current Investigations and the Future. *Front Immunol*, 2022. 13:
749 p. 817296.

750 7. Taraseviciute, A., et al., Chimeric Antigen Receptor T Cell-Mediated
751 Neurotoxicity in Nonhuman Primates. *Cancer Discov*, 2018. 8(6): p. 750-763.

752 8. Xu, S., et al., Immunotherapy for glioma: Current management and
753 future application. *Cancer Lett*, 2020. 476: p. 1-12.

754 9. Brown, C.E., et al., Regression of Glioblastoma after Chimeric Antigen
755 Receptor T-Cell Therapy. *N Engl J Med*, 2016. 375(26): p. 2561-9.

756 10. Lombardi, G., et al., Regorafenib compared with lomustine in patients
757 with relapsed glioblastoma (REGOMA): a multicentre, open-label, randomised,
758 controlled, phase 2 trial. *Lancet Oncol*, 2019. 20(1): p. 110-119.

759 11. Stupp, R., et al., NovoTTF-100A versus physician's choice
760 chemotherapy in recurrent glioblastoma: a randomised phase III trial of a novel
761 treatment modality. *Eur J Cancer*, 2012. 48(14): p. 2192-202.

762 12. Braud, V.M., et al., HLA-E binds to natural killer cell receptors
763 CD94/NKG2A, B and C. *Nature*, 1998. 391(6669): p. 795-9.

764 13. Mali, P., et al., RNA-guided human genome engineering via Cas9.
765 *Science*, 2013. 339(6121): p. 823-6.

766 14. Cong, L., et al., Multiplex genome engineering using CRISPR/Cas
767 systems. *Science*, 2013. 339(6121): p. 819-23.

768 15. Cox, D.B., R.J. Platt, and F. Zhang, Therapeutic genome editing:
769 prospects and challenges. *Nat Med*, 2015. 21(2): p. 121-31.

770 16. Choo, S.Y., The HLA system: genetics, immunology, clinical testing,
771 and clinical implications. *Yonsei Med J*, 2007. 48(1): p. 11-23.

772 17. Xu, H., et al., Targeted Disruption of HLA Genes via CRISPR-Cas9
773 Generates iPSCs with Enhanced Immune Compatibility. *Cell Stem Cell*, 2019.

774 24(4): p. 566-578 e7.

775 18. Kitano, Y., et al., Generation of hypoimmunogenic induced pluripotent
776 stem cells by CRISPR-Cas9 system and detailed evaluation for clinical
777 application. *Mol Ther Methods Clin Dev*, 2022. 26: p. 15-25.

778 19. Torikai, H., et al., Toward eliminating HLA class I expression to
779 generate universal cells from allogeneic donors. *Blood*, 2013. 122(8): p. 1341-
780 9.

781 20. Torikai, H., et al., Genetic editing of HLA expression in hematopoietic
782 stem cells to broaden their human application. *Sci Rep*, 2016. 6: p. 21757.

783 21. Ren, J., et al., Multiplex Genome Editing to Generate Universal CAR T
784 Cells Resistant to PD1 Inhibition. *Clin Cancer Res*, 2017. 23(9): p. 2255-2266.

785 22. Depil, S., et al., 'Off-the-shelf' allogeneic CAR T cells: development and
786 challenges. *Nat Rev Drug Discov*, 2020. 19(3): p. 185-199.

787 23. Duygu, B., et al., HLA Class I Molecules as Immune Checkpoints for
788 NK Cell Alloreactivity and Anti-Viral Immunity in Kidney Transplantation.
789 *Front Immunol*, 2021. 12: p. 680480.

790 24. Sun, W., et al., Universal chimeric antigen receptor T cell therapy - The
791 future of cell therapy: A review providing clinical evidence. *Cancer Treat Res*
792 *Commun*, 2022. 33: p. 100638.

793 25. Meril, S., et al., Targeting glycosylated antigens on cancer cells using
794 siglec-7/9-based CAR T-cells. *Mol Carcinog*, 2020. 59(7): p. 713-723.

795 26. Ouyang, H., et al., Baseline and early changes in the neutrophil-
796 lymphocyte ratio (NLR) predict survival outcomes in advanced colorectal
797 cancer patients treated with immunotherapy. *Int Immunopharmacol*, 2023. 123:

798 p. 110703.

799 27. Rui, Y. and J.J. Green, Overcoming delivery barriers in immunotherapy
800 for glioblastoma. *Drug Deliv Transl Res*, 2021. 11(6): p. 2302-2316.

801 28. Choi, B.D., et al., Intraventricular CARv3-TEAM-E T Cells in
802 Recurrent Glioblastoma. *N Engl J Med*, 2024. 390(14): p. 1290-1298.

803 29. Bagley, S.J., et al., Intrathecal bivalent CAR T cells targeting EGFR and
804 IL13Ralpha2 in recurrent glioblastoma: phase 1 trial interim results. *Nat Med*,
805 2024. 30(5): p. 1320-1329.

806 30. Brown, C.E., et al., Locoregional delivery of IL-13Ralpha2-targeting
807 CAR-T cells in recurrent high-grade glioma: a phase 1 trial. *Nat Med*, 2024.
808 30(4): p. 1001-1012.

809 31. Brown, C.E., et al., Bioactivity and Safety of IL13Ralpha2-Redirected
810 Chimeric Antigen Receptor CD8+ T Cells in Patients with Recurrent
811 Glioblastoma. *Clin Cancer Res*, 2015. 21(18): p. 4062-72.

812 32. Haque, W., et al., Patterns of management and outcomes of unifocal
813 versus multifocal glioblastoma. *J Clin Neurosci*, 2020. 74: p. 155-159.

814 33. Chamberlain, M.C., et al., Pharmacokinetics of intralumbar DTC-101
815 for the treatment of leptomeningeal metastases. *Arch Neurol*, 1995. 52(9): p.
816 912-7.

817 34. Mackensen, A., et al., CLDN6-specific CAR-T cells plus amplifying
818 RNA vaccine in relapsed or refractory solid tumors: the phase 1 BNT211-01
819 trial. *Nat Med*, 2023. 29(11): p. 2844-2853.

820 35. Kalbasi, A., et al., Potentiating adoptive cell therapy using synthetic IL-
821 9 receptors. *Nature*, 2022. 607(7918): p. 360-365.

822 36. O'Rourke, D.M., et al., A single dose of peripherally infused EGFRvIII-
823 directed CAR T cells mediates antigen loss and induces adaptive resistance in
824 patients with recurrent glioblastoma. *Sci Transl Med*, 2017. 9(399).

825 37. Brown, M.P., L.M. Ebert, and T. Gargett, Erratum: Clinical chimeric
826 antigen receptor T-cell therapy: a new and promising treatment modality for
827 glioblastoma. *Clin Transl Immunology*, 2021. 10(8): p. e1331.

828 38. Davila, M.L., et al., Efficacy and toxicity management of 19-28z CAR
829 T cell therapy in B cell acute lymphoblastic leukemia. *Sci Transl Med*, 2014.
830 6(224): p. 224ra25.

831 39. Majzner, R.G., et al., GD2-CAR T cell therapy for H3K27M-mutated
832 diffuse midline gliomas. *Nature*, 2022. 603(7903): p. 934-941.

833 40. Waxman, E.S. and D. Lee Gerber, Pseudoprogression and
834 Immunotherapy Phenomena. *J Adv Pract Oncol*, 2020. 11(7): p. 723-731.

835 41. Brandes, A.A., et al., Temozolomide in patients with glioblastoma at
836 second relapse after first line nitrosourea-procarbazine failure: a phase II study.
837 *Oncology*, 2002. 63(1): p. 38-41.

838 42. Chang, S.M., et al., Temozolomide in the treatment of recurrent
839 malignant glioma. *Cancer*, 2004. 100(3): p. 605-11.

840 43. Brada, M., et al., Multicenter phase II trial of temozolomide in patients
841 with glioblastoma multiforme at first relapse. *Ann Oncol*, 2001. 12(2): p. 259-
842 66.

843 44. Yung, W.K., et al., A phase II study of temozolomide vs. procarbazine in
844 patients with glioblastoma multiforme at first relapse. *Br J Cancer*, 2000. 83(5):
845 p. 588-93.

846 45. Moen, M.D., Bevacizumab: in previously treated glioblastoma. Drugs,
847 2010. 70(2): p. 181-9.

848 46. Kim, M.M., Y. Umemura, and D. Leung, Bevacizumab and
849 Glioblastoma: Past, Present, and Future Directions. Cancer J, 2018. 24(4): p.
850 180-186.

851 47. Chen, Z., Y. Hu, and H. Mei, Advances in CAR-Engineered Immune
852 Cell Generation: Engineering Approaches and Sourcing Strategies. Adv Sci
853 (Weinh), 2023. 10(35): p. e2303215.

854 48. Martinez, M. and E.K. Moon, CAR T Cells for Solid Tumors: New
855 Strategies for Finding, Infiltrating, and Surviving in the Tumor
856 Microenvironment. Front Immunol, 2019. 10: p. 128.

857

858 **Acknowledgments**

859 This work was supported by foundation of Chongqing International Institute for
860 Immunology (2021YZH01 to X-Y. S), National Natural Science Foundation of China
861 (No. 82173279, 82472981 to Y-L.H), and National Science and Technology Resource
862 Sharing Service Platform (YCZYPT[2020]06-1 to Y-L.H), Suzhou Medical and Health
863 Innovation Project (CXYJ2024A05 to Y-L.H), Suzhou Industrial Park Healthcare
864 Talent Support Initiative (2024-54 to Y-L.H), Gusu Talent Program(2024-105 to Y-L.H),
865 and the National Natural Science Foundation of China (82350112 to H-B.L.). These
866 funders provided support for study design, data collection and analysis, and manuscript
867 preparation.

868 We thank the patients who participated in this trial and their families for making this
869 trial possible; the study team, caregivers, and other personnel for their individual
870 professional assistance; and the staff of the department of technology, T-MAXIMUM

871 Pharmaceuticals (Suzhou) Co., Ltd., for technical support. We also extend our gratitude
872 to Yijin Li and Xiu Zhao from T-MAXIMUM Pharmaceuticals for their valuable
873 insights and fruitful discussions that significantly contributed to the development of this
874 study.

875

876 **Author contributions**

877 Y.H., X.S., and Y.Wu conceived the clinical trial concept. ZhongW., X.L., ZhiminW., J.
878 L., X. Y., H.Z. and Z.X. enrolled patients in the clinical trial, X.Z., X.R., Y.L., X.L., J.S.,
879 Z.B. and L.H. evaluated toxicity and participated in critical discussions, as well as
880 manuscript writing and editing. W.G. performed the pathology assessments. H.L. and
881 L.W. performed the immunological assays. X.J., YangZ., and J.C. conducted formal
882 analysis, data visualization, writing—original draft and writing—review and editing.
883 X.S., YuZ., J.G., X.M., and Y.Wang obtained resources, managed data, performed
884 project administration, and performed writing—review and editing. Y.Wu and Y.H.
885 contributed to writing—original draft, writing—review and editing, funding acquisition,
886 formal analysis, and data curation.

887

888 **Competing interests Statement**

889 All authors have no competing interests.

Fig. 1 Characterization of allogeneic UCAR-T cells *In vitro* and *In vivo*.

a, Expression of TCR and HLA-I T cells in double-knockout T cells. **b**, Evaluation of T cell activities in double-knockout CAR-T cells. **c**, NK cells were mixed with K562 cells or UCAR-T cells or WT T cells at a 2:1 ratio for 24 h. Data are from 1 of 3 similar experiments. **d**, GvHD modeling assay to validate the *HLA-TRAC* dual-editing strategy: MT026 cells (TCR-knockout UCAR-T) showed no proliferation when co-cultured with allogeneic PBMCs for 120 h, contrasting with significant expansion in conventional CAR-T (TCR-intact) and WT T cells. **e**, Cell count of CAR-T cells with different knockout strategies co-cultured with allogeneic PBMCs (NK-cell depleted) for 12 days was detected. **f**, Cell count of cells with distinct knockout strategies co-cultured with allogeneic NK cells for 24 h was measured. Representative data from a single donor are shown. Each sample was set with 3 technical replicates, and the experiment was performed at least in 3 biologically independent repeats. Data from all three donors are provided in **Supplementary Table 1**. Source data are provided as a Source Data file.

Fig. 2 *In vitro* and *in vivo* anti-tumor effect of IL-13Ra2 allogeneic UCAR-T.

a, The U251 tumor cells were co-cultured with MT026 (Anti-IL-13Ra2 allogeneic UCAR-T) cells from two different donors or CAR-T cells, and the specific killing of tumor cells was measured by flow cytometry over 24 h, with 3 biologically independent experiments for each sample. Error bars represent mean \pm SD. n = 3 for CAR-T and MT026 at effector:target ratios of 0.5:1 (CAR-T mean = 38.75, MT026 mean = 39.81), 1:1 (CAR-T mean = 51.28, MT026 mean = 52.19), 2:1 (CAR-T mean = 60.78, MT026 mean = 62.09), 5:1 (CAR-T mean = 70.83, MT026 mean = 68.94), and 10:1 (CAR-T mean = 79.86, MT026 mean = 79.03). Differences are not significant (ns), calculated by two-way ANOVA. **b**, Fluorescence images of the GFP-labeled organoids co-cultured with IL-13Ra2 CAR-T cells at various E: T ratios for 0, 12, 24, 48, and 72 h. Scale bar, 3000 μ m; **c**, Quantification of the relative fluorescence intensity of GFP-labeled organoids in panel B was performed using Image J software, with 4 biologically independent samples for each sample. Error bars represent \pm SDs. ****p < 0.0001 calculated by two-way ANOVA. **d**, Schematic illustration of the *in vivo* experiment; **e**, Kaplan-Meier survival curves of the Patient-Derived Orthotopic Xenograft (PDOX) mouse models, which were intratumorally injected with IL-13Ra2 CAR-T cells in panel d, n=8 mice per group. Significance of difference was determined by two-tailed log rank test. ****p < 0.0001. **f**, Representative bioluminescent images (BLI) of the Patient-Derived Orthotopic Xenograft (PDOX) mouse models, which were intratumorally injected with IL-13Ra2 CAR-T cells in panel d, n=8 mice per group. **g**, Tumor burden measured by BLI in mice of each treatment group in panel d, n=8 mice per group. Error bars represent \pm SDs. **p = 0.0031, ****p < 0.0001 calculated by two-way ANOVA. Source data are provided as a Source Data file.

Fig. 3 Pharmacokinetic Characteristics of MT026.

a and b, CAR DNA copies and IL-6 concentrations in cerebrospinal fluid of MT026 before and 1 day after each administration. Baseline value is defaulted to zero. The administration interval is approximately 1 month. **c**, Change of multiple cytokines in CSF before and after the 4th MT026 administration in Patient 005. **d**, IL-6 concentrations in cerebrospinal fluid and blood of MT026 after different administration. Error bars represent \pm SDs. Biological replicates: for CSF, n = 3 per group for 1st-4th, n = 1 for 5th; for PB, n = 2 per group for 1st-4th, n = 1 for 5th. **e**, Change of blood lymphocyte count with treatment of MT026 in the 5 patients. **f**, Change of neutrophils to lymphocytes ratio in blood with treatment of MT026 in the 5 patients. Source data are provided as a Source Data file

Fig. 4 Efficacy of MT026 Therapy.

a, CONSORT Flow diagram. **b**, Study Schema. **c**, Disease development over time in the five patients. **d**, The ratio of cross-sectional area of the target lesion relative to baseline at each assessment point as the rate of tumor growth. Black, red, orange, and purple triangles indicate IL-13R α 2-, B7-H3-, HER2-, and EGFR-targeted CAR-T therapies, respectively. **e**, MRI assessment of tumor size at baseline and best overall response after intra-thecal, via lumbar puncture injection of MT026 in the five patients. The number above the MRI image represents the exact scanning time, the characters on the right side of the image indicate the cycle count, the best evaluation result, and the number of days after the first administration. C represents cycle, CR = complete response, PR = partial response, SD = stable disease. **f**, The best percent change from baseline in tumor size in the five patients, where the data cutoff date was July 6, 2022 (median follow-up, 8.4 months). Source data are provided as a Source Data file.

Fig. 5 Schematic diagram of anti-IL-13R α 2 allogeneic UCAR-T knockout TCR and HLA-I of T cells by gene editing technology.

This figure summarizes the genome editing strategy for engineering universal chimeric antigen receptor (CAR)-T cells, alongside the functional goals of these modifications.

Central Schematic (Edited T Cell): The cartoon depicts a T cell modified via CRISPR/Cas9 (scissors symbols at TRAC and HLA-I loci). Key edits include: TRAC Knockout (Label ①): Disruption of the TRAC locus (encoding TCR α -chain) to eliminate endogenous T cell receptor (TCR) expression. HLA-I Knockout (Label ②): Inactivation of HLA-I α -chain (HLA-A/B/C) to ablate HLA-I surface presentation. CAR Insertion (Label ③): Introduction of a CAR to equip the cell with tumor-targeting specificity. **Adjacent Panels:** Our Editing Strategy lists the three core manipulations: TCR (TRAC) knockout, HLA-I α -chain knockout, and CAR insertion. **Main Objective of Edit** outlines the strategy's functions: preventing graft-versus-host disease (GvHD; via TCR knockout), mitigating T/NK-mediated rejection (via HLA-I knockout), and directing tumor killing (via CAR).

Table 1. Patient Characteristics, Prior Therapies, Study Drug Exposures, and Clinical Outcome

Patient ID	MT026-001	MT026-002	MT026-003	MT026-004	MT026-005
Age (years)	50	63	52	57	45
Male (M)/Female (F)	M	F	F	F	F
KPS Score	60	40	60	90	50
IL-13R α 2 Expression Level	Medium	High	Medium	Medium	Medium
Unmethylated MGMT Promoter Status	+	+	+	+	+
Wild Type IDH1/2 Genetic Profile	+	+	+	+	+
Number of Cycles of Prior Conventional Treatment (Surgery, Radiation, Temozolomide)	1-2	1-2	1-2	1-2	1-2
Study Drug Exposure (Number of Infusions)	5	9	6	4	5
Treatment Length in Months	3.6	7.9	4.9	2.6	4.0
Time to Death from Day 1 (months)	7.6	17.2	8.3	10.5	5.7
Time from Recurrence to Day1 (months)	5.3	16.0	0.9	3.2	7.3
Survival Time from Recurrence (months)	12.8	33.2	9.2	13.7	13.1

Note:

Karnofsky Performance Score (KPS)

Table 2. Study of Drug-Related Adverse Events and Reported Lab Abnormalities

Study of Drug-Related Adverse Events	No. of subjects (%)	CTCAE grading
Fever	4 (80)	1-2
Hypoxia	2 (40)	1-2
Vomiting	2 (40)	1-2
Headache	1 (20)	1
Reported Lab abnormalities	No. of subjects (%)	CTCAE grading
Increased CSF IL-6	5 (100)	NA
Increased CSF total protein	4 (80)	NA
Increased CSF lactate dehydrogenase	3 (60)	NA
Increased serum CRP	3 (60)	NA
Increased serum IL-6	2 (40)	NA
Lymphocyte count decreased	5 (100)	1-2
Leukocytosis	3 (60)	1-2
White blood cell decreased	1 (20)	1

Table 3. MT026 Treatment via Intrathecal Delivery was Safe and Tolerated in Patients with Recurrent High-Grade Glioma

MT026 1.0-3.0X10⁷	
n=5	
AE Grade 3 or greater	No
Study drug related AE Grade 3 or greater	No
AE leading to study drug discontinuation	No
SAE	No
Death	5 (100%)
Lab abnormality Grade 3 or greater	No
CRS Grade 3 or greater	No
ICANS Grade 3 or greater	No
GVHD	No
Infection	No
Cytopenia Grade 3 or greater	No

Note: All data are n (%);

CRS: Cytokine Release Syndrome; ICANS: Immune Effector Cell-Associated Neurotoxicity

GVHD: Graft Versus-Host Disease; AE: Adverse Event; SAE: Serious Adverse Event

Table 4. Overall efficacy summary. *

Variable	Results (N=5)
Best overall response – no. (%) †	
Complete response	1 (20.0)
Partial response	3 (60.0)
Stable disease	1 (20.0)
Progressive disease	0 (0)
Objective response	
No. of patients	4
Percent (95% CI)	80 (37.6-96.4)
Disease control	
No. of patients	5
Percent (95% CI)	100 (56.6-100)
Time to response – mo	
Mean time to response (95% CI)	2.2 (1.3-3.0)
Min time to response	1.2
Duration of response – mo	
Mean duration of response (95% CI)	3.4 (1.6-5.3)
Max duration of response	5.2
Progression-free survival	
Mean progression-free survival (95% CI) - mo	4.7 (3.0-6.3)
Max progression-free survival - mo	10.1
6-month progression-free survival rate (95% CI) - %	20.0 (34.6-100)
Overall survival	
Mean overall survival (95% CI) - mo	8.3 (6.7-9.8)
Max overall survival - mo	17.2
12-month overall survival rate (95% CI) - %	20.0 (3.5-100)
Survival duration from recurrence	
Mean survival duration from recurrence (95% CI) - mo	13.1 (12.6-13.6)
Max survival duration from recurrence - mo	33.2
Rate of 12-month survival duration from recurrence (95% CI) - %	80.0 (51.6-100)

* The data cutoff date for efficacy end points was July 6, 2022 unless otherwise noted. CI denotes confidence interval, and mo months.

† Best overall response was assessed according to the Immunotherapy Response Assessment in Neuro-Oncology (iRANO).

Table 5. Baseline demographic and clinical characteristics.

Patient ID	Sex/age	KPS	IL-13R α 2 score	antigen expression in tumor tissue	Prior temozolomide before recurrence	No. of injection before BOR
MT026-001	M/50	60	Medium		Yes	1
MT026-002	F/63	40	High		Yes	5
MT026-003	F/52	60	Medium		Yes	3
MT026-004	F/57	90	Medium		Yes	5
MT026-005	F/45	50	Medium		Yes	3

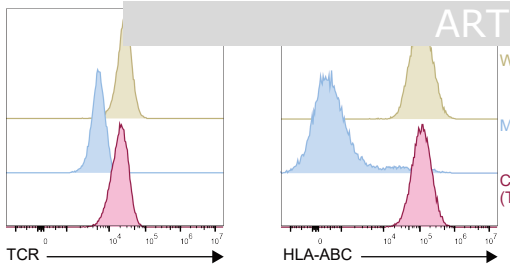
Editorial summary

Off-the-shelf, on-demand allogeneic CAR-T cells could represent a therapeutic alternative to autologous products for cancer therapy. Here the authors report the preclinical characterization of off-the-shelf CRISPR-Cas9– edited IL-13R α 2-specific allogeneic universal CAR-T cells and the results of a first-in-human phase I trial in patients with high-grade glioma.

Peer Review Information: *Nature Communications* thanks the anonymous reviewer(s) for their contribution to the peer review of this work. A peer review file is available.

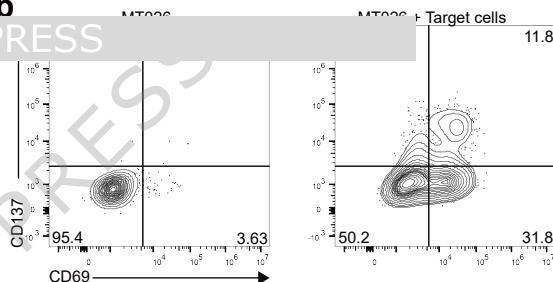
ARTICLE IN PRESS

a

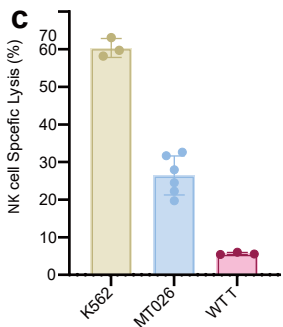


Conventional CAR-T
(TCR+HLA-I+ CAR-T)

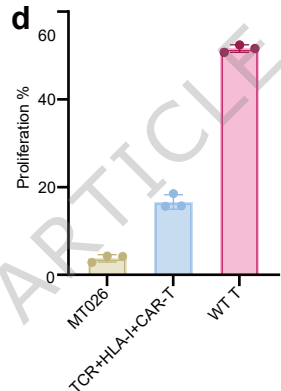
b



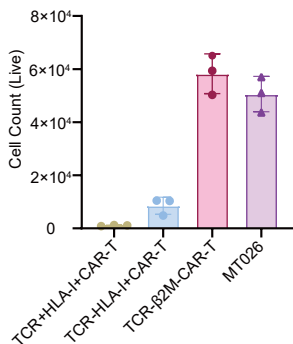
c



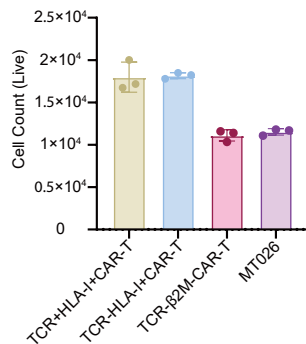
d

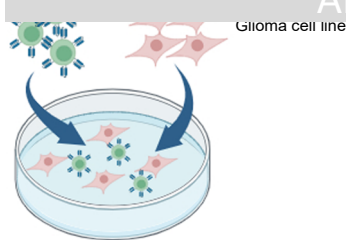


e

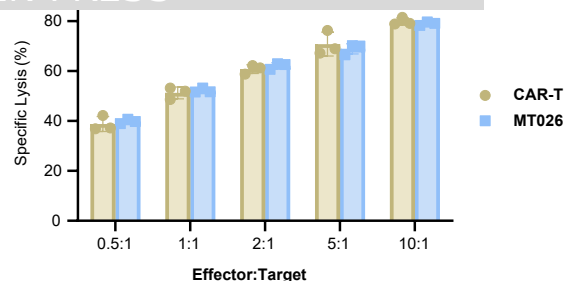
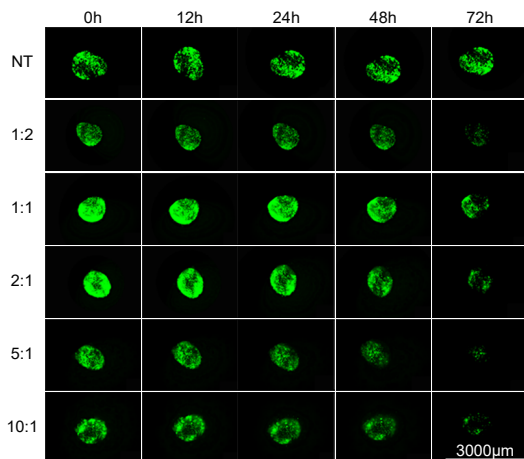
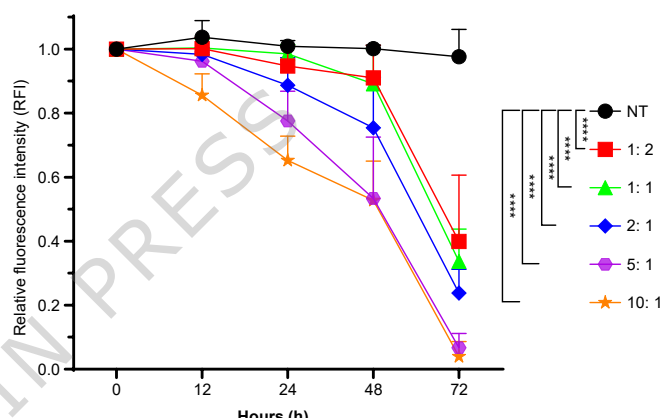
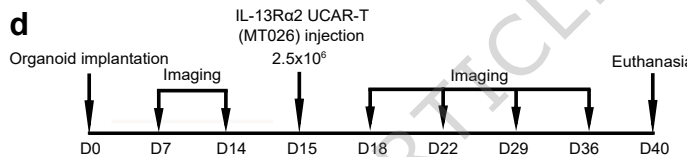
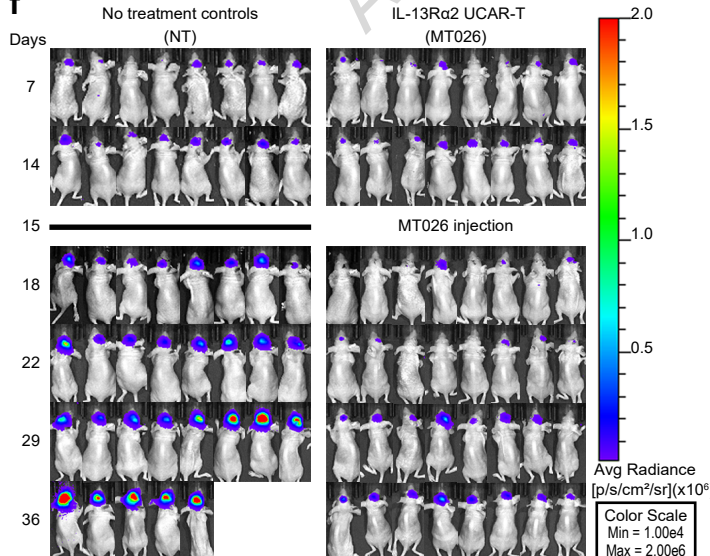
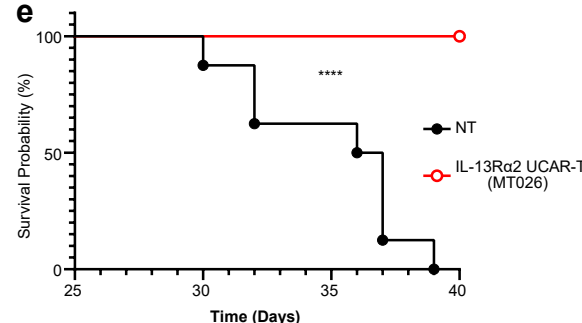
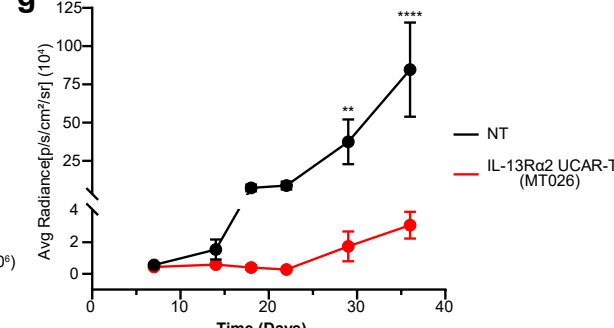


f



aIL-13Ra2 UCAR-T
(MT026)

ARTICLE IN PRESS

**b****c****d****f****e****g**

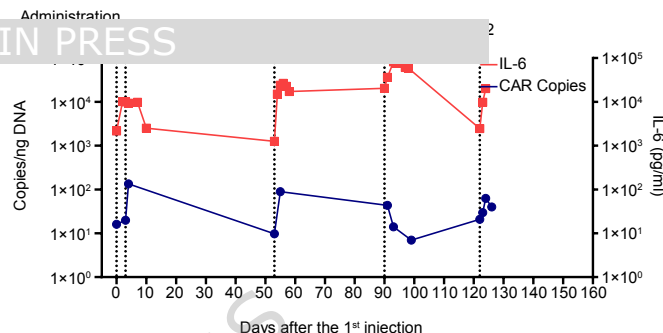
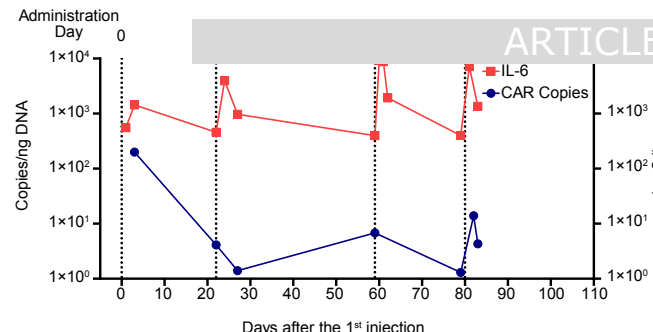
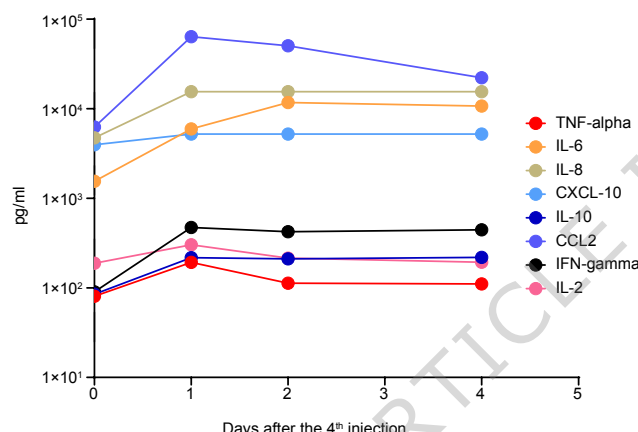
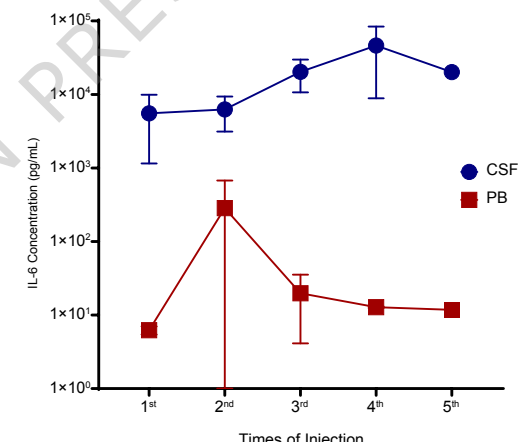
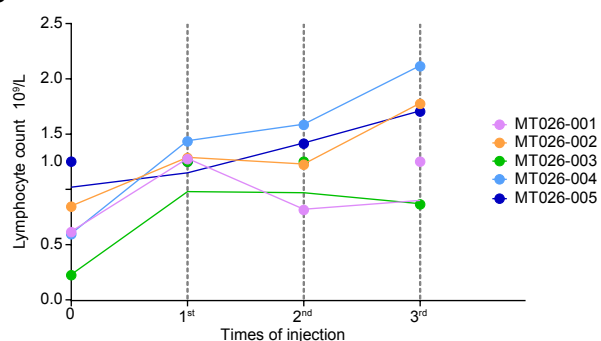
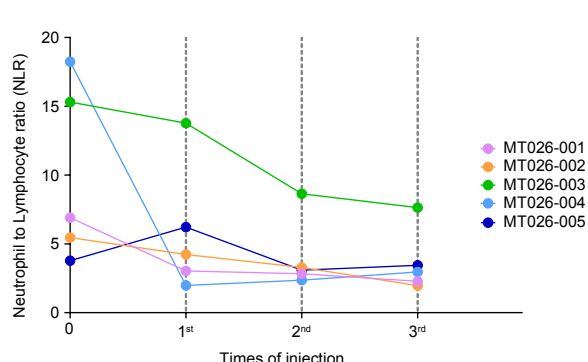
a

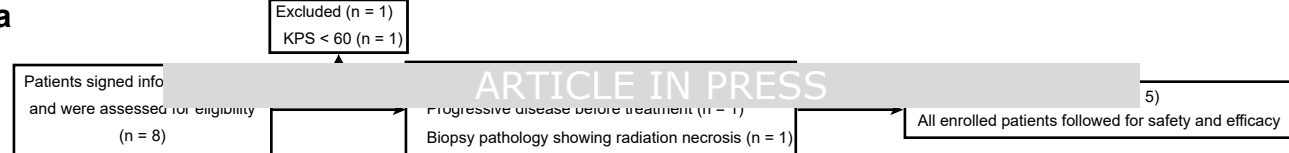
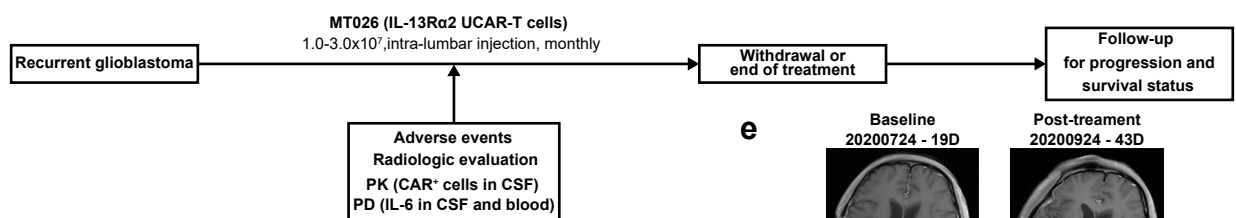
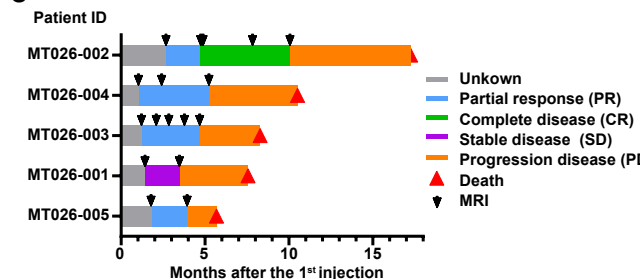
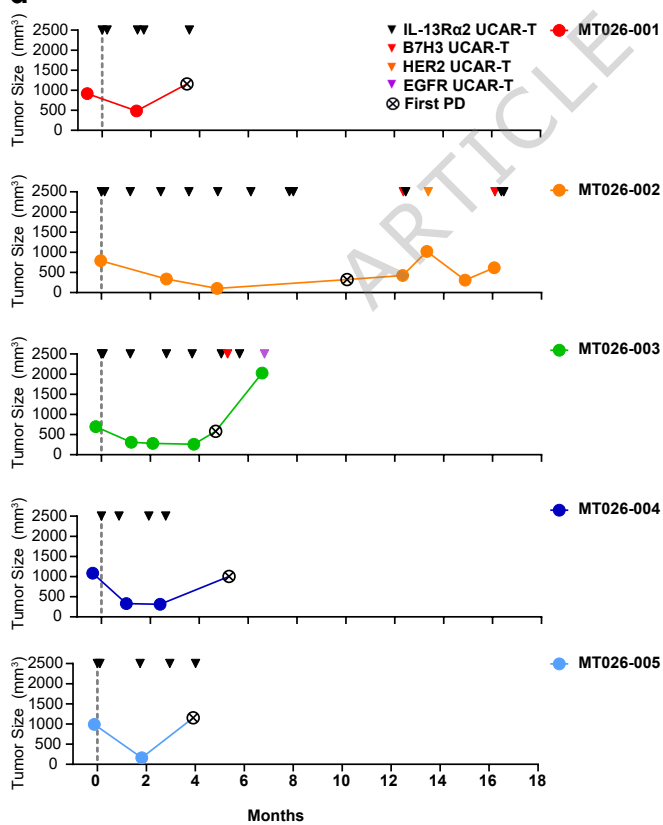
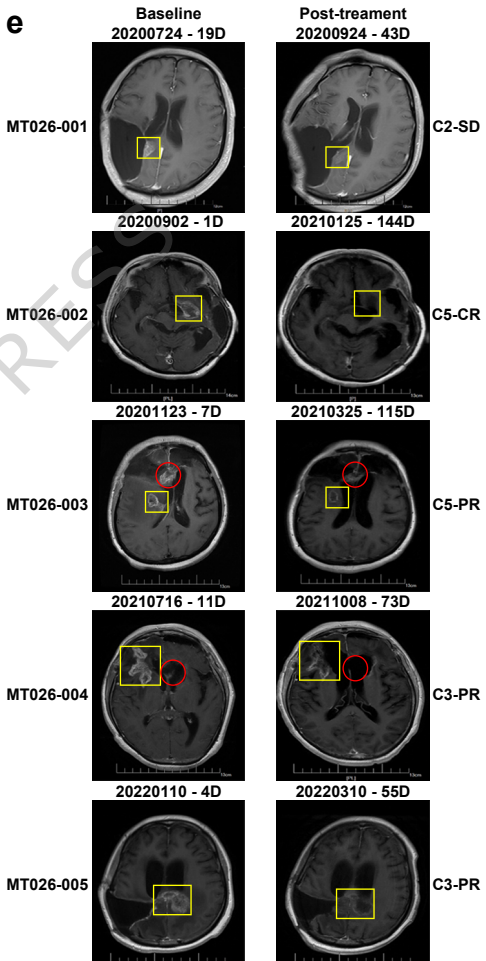
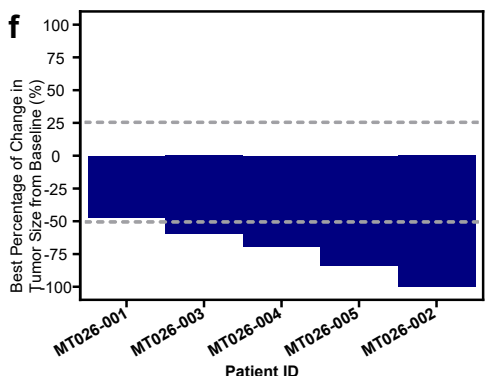
MT026-004

b

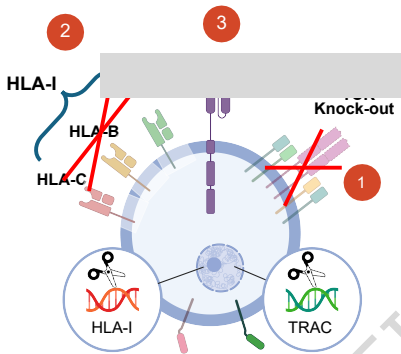
MT026-005

ARTICLE IN PRESS

**c****d****e****f**

a**b****c****d****e****f**

ARTICLE IN PRESS



1 Knockout endogenous TCR

2 Knockout alpha chain of
HLA-I instead of B2M

3 CAR insertion

of Edit

Prevent Graft-versus-Host
Disease (GvHD)

Mitigate T and
NK-mediated rejection

Direct T cell for tumor killing